Determining robot's maximum dynamic load carrying capacity in point-to-point motion by applying limitation of joints' torque

H. R. Shafei[1], M. Bahrami[2], A. Kamali E[3] and A. M. Shafei[4*]

1- Mechanic Engineering Department, Amirkabir University of Technology, Tehran, Iran
2- Mech. Eng. Amirkabir University of Technology, Tehran, Iran
3- Mech. Eng. Amirkabir University of Technology, Tehran, Iran
4- Department of Mechanical Engineering, Shahid Bahonar University of Kerman, Kerman, Iran
Corresponding Author: A. M. Shafei

A B S T R A C T

   This article seeks to determine a two-link robot's maximum dynamic load carrying capacity (DLCC) in a point-to-point motion by applying torque limits on its joints. The method presented here is based on open-loop optimal control and it uses indirect approach to derive optimality conditions. The Pontryagin's minimum principle (PMP) has been used to obtain the optimality conditions that it leads to a two-point boundary value problem (TPBVP). Two sets of differential equations and one algebraic equation are obtained which are solved by using BVP4C command in MATLAB software. In this paper, a robot's DLCC in a point-to-point motion has been determined in two ways. In the first case, no torque limit constraint has been considered in the Hamiltonian function for the joints; while in the second case, this constrain has been incorporated into the Hamiltonian function and it appears in the equations obtained by using PMP which causes this constrain to show up in the state and costate equations. In both cases, simulations have been performed. The simulation results indicate that when a torque limit constraint is considered in the Hamiltonian function, the angular positions and velocity of robot's joints are the same, but the torque of joints are different.

Keywords: Robotic arm; Maximum load carrying capacity; Optimum trajectory; Torque limits.

INTRODUCTION

   The dynamic load carrying capacity of a robot is defined as "the maximum load that a robotic system can carry provided that the motors' torques do not exceed the saturation limits". DLCC is one of the criteria for selection of robotic systems. Generally, two methods (direct and indirect) exist for solving the problem of DLCC (1-2).

Direct method:
   This method is based on the discretization of a system's dynamic variables (state and control variables) that leads to a parameter optimization problem. Then, linear optimization methods (3), nonlinear optimization methods (4), evolutionary techniques (5) or Stochastic Techniques (6) are employed to obtain the optimal values of the parameters. The variables may be classified as state variables, control variables or both (7). The linearizing procedure in direct method and its convergence is a challenging issue, especially when nonlinear terms are large and fluctuating (7, 8). In this way, the obtained answer is an approximate solution which is directly related to the order of polynomial function. Wang et al. (4) have solved an optimal control problem by using 'Bspline' functions to calculate the maximum load of a fixed manipulator. The main idea of their research is to discretization the joints trajectories by using Bspline functions and then determining the parameters through nonlinear optimization so as to obtain a local minimum which yields the constraints. A shortcoming of this method is that it limits the solution to a fix-order polynomial (9).

Iterative Linear Programming (ILP) is another direct method by which a trajectory optimization problem becomes a linear programming problem. The first formulation of this method for calculating the maximum load carried by a simple robot has been provided by Wang and Ravani (4). The linearization operation in the ILP method and its convergence towards the optimal path are difficult tasks, especially when a system has a large degree of freedom or it contains large and fluxionary nonlinear terms.

Korayem and Ghariblu used the ILP method to determine the DLCC of a robotic arm with elastic links and also with elastic joints for point-to-point motion and also for motion along a specified trajectory (10, 11). They formulated the DLCC problem as an optimization problem and then employed the ILP method (a direct method) to solve the problem. In their work the boundary conditions are hardly satisfied and there is an almost 10% error in the final solution.

Indirect method:

This is another method for obtaining the optimal trajectory of the maximum payload. The indirect method, which is based on the PMP, was initially used to solve optimal control problems (12). This method was employed to solve the problems of obtaining the minimum time of motion along specified trajectories (13). In this method, the optimality conditions are extracted as a set of differential equations which, along with the given boundary conditions, form a TPBVP. These sets of differential equations are solved by means of numerical techniques such multiple shooting method (14) or Gradient method (GM) (15). By solving this problem an exact solution can be found. Through this approach, the optimal trajectories for fixed and redundant robots can be calculated by considering different objective functions such as the maximization of the load carrying, minimization of the movement time and minimization of torque, etc. By applying an indirect method which yielded a TPBVP, Korayem and Nikoobin obtained a two-link robot's DLCC in a point-to-point task (16).

In this article, first, a two-link robot's DLCC is determined by applying torque constraint on the joints (as was previously obtained by Korayem and Nikoobin (16)). Then by revising the method used in Ref. (16) and considering the application of dynamic torque, the problem is resolved and then the obtained results are compared to each other.

So, the rest of the paper is organized as follows. In Section 2 the mathematical modeling of the problem will be described. Section 3 is devoted to extract optimality conditions and the TPBVP. In Section 4, first, a two-link robot's DLCC is obtained using the method applied in Ref. (16), and then this problem is resolved by assuming dynamic torque of each joint. And finally in Section 5 the conclusions from the present work are summarized.

Problem formulation:
The dynamical model of a robot is described in the Lagrangian formulation as:

$$D(q)\ddot{q} + C(q,\dot{q})\dot{q} + G(q) = U \qquad (1)$$

where U is the torque vector of the joints, D is the inertia matrix, C represents the centripetal and Coriolis forces and G expresses the effects of gravity (2). By using the state vector as:

$$X = \begin{bmatrix} X_1 \\ X_2 \end{bmatrix} = \begin{bmatrix} q \\ \dot{q} \end{bmatrix} \qquad (2)$$

In the state space form, Eq. (1) is expressed as:

$$\dot{X} = F(X,U) \qquad (3)$$

where F is defined as:

$$F = \begin{bmatrix} F_1 \\ F_2 \end{bmatrix} = \begin{bmatrix} X_2 \\ N(X_1, X_2) + Z(X_1)U \end{bmatrix} \qquad (4)$$

$$N(X_1, X_2) = -D^{-1}(X_1)[C(X_1, X_2)X_2 + G(X_1)]$$
$$Z(X_1) = D^{-1}(X_1) \qquad (5)$$

Thus, the dynamic equations of motion in state-space are obtained.

Expressing the problem of optimal control

Supposing that a proper joint torque value exists in the Ω space ($U^*(t) \in \Omega$), the goal is to determine $U^*(t)$ so that the general cost function is minimized as follows:

$$J_o(U, m_p) = \underbrace{\frac{1}{2}\|e_p(t_f)\|^2 + \frac{1}{2}\|e_v(t_f)\|^2}_{h(X(t_f), t_f)} + \int_{t_0}^{t_f} L(X, U, m_p)dt \quad (6)$$

where e_p, e_v and L are defined as

$$e_p(t_f) = X_1(t_f) - X_{1f}$$
$$e_v(t_f) = X_2(t_f) - X_{2f} \quad (7)$$

$$L(X, U, m_p) = \frac{1}{2}\|X_1\|_{W_1}^2 + \frac{1}{2}\|X_2\|_{W_2}^2 + \frac{1}{2}\|U\|_R^2 \quad (8)$$

where t_0 and t_f are the initial and final times and m_p is the maximum load that can be carried by the robotic system. L represents a uniform and derivable function. W_p and W_v are symmetric, positive semi-definite matrices. W_1, W_2 and R are symmetric positive definite matrix. X_{1f} and X_{2f} are the desired values for the position and angular velocity of joints, respectively. The cost function determined by Eq. (6) through Eq. (8) is minimized within the entire trajectory of the robot. In Eq. (6), the first and second terms are related to minimization of errors of a robot's position and velocity at the final point, respectively. Eq. (8) is related to minimization of a joint's angular position, velocity and torque throughout the entire trajectory of the robot.

$$X_1(0) = X_{10}, \quad X_2(0) = X_{20}$$
$$X_1(t_f) = X_{1f}, \quad X_2(t_f) = X_{2f} \quad (9)$$

Eq. (9) defines the angular position and angular velocity of each joint at the initial and final point. The permissible bound of each motor can express as follows:

$$\overline{U} = \{U^- \leq U \leq U^+\} \quad (10)$$

In indirect method, by introducing a costate vector (ψ), the Hamiltonian function is expressed as:

$$H(X, U, \Psi, m_p, t) = L(X, U, m_p) + \psi^T(t)F(X, U, m_p) \quad (11)$$

where, based on the PMP, there exists a non-zero costate vector for a specified m_p payload for which the following optimality conditions must be satisfied.

$$\dot{X}^*(t) = \frac{\partial H}{\partial \psi}(X^*, U^*, \psi^*, m_p, t) \quad (12)$$

$$\dot{\psi}^*(t) = -\frac{\partial H}{\partial X}(X^*, U^*, \psi^*, m_p, t) \quad (13)$$

$$0 = \frac{\partial H}{\partial U}(X^*, U^*, \psi^*, m_p, t) \tag{14}$$

$$\left[\frac{\partial h}{\partial X}\left(X^*(t_f), t_f\right) - \psi^*(t_f)\right]^T \delta X_f +$$

$$\left[H\left(X^*(t_f), U^*(t_f), \psi^*(t_f), t_f\right) + \frac{\partial h}{\partial t}\left(X^*(t_f), t_f\right)\right]\delta t_f = 0 \tag{15}$$

In these relations, the symbol (*) indicates the extremals of the states, costates and controls. The obtained optimality condition is related to a state in which the state variables and the joints' torque values are not bounded. In order to apply a constraint on the control variables, we should consider the following:

$$H(X^*, U^*, \psi^*, t) \leq H(X^*, \psi^*, \overline{U}, t) \tag{16}$$
$$\textit{for all } t \in \begin{bmatrix} t_0 & t_f \end{bmatrix} \textit{and } U \in \overline{U} \tag{17}$$

In Eq. (16), $\overline{U}$ is a permissible control value. By assuming ψ to be a costate vector, the optimality conditions are obtained as Eq. (18) to Eq. (21).

$$\dot{X}(t) = \begin{bmatrix} \dot{X}_1 \\ \dot{X}_2 \end{bmatrix} = \begin{bmatrix} X_2 \\ N(X_1, X_2) \end{bmatrix} + \begin{bmatrix} 0 \\ Z(X_1) \end{bmatrix} U \tag{18}$$

$$\dot{\psi}(t) = -\begin{bmatrix} \frac{\partial L^T}{\partial X_1} + \frac{\partial}{\partial X_1}[N(X) + Z(X_1)U]^T \psi_2 \\ \frac{\partial L^T}{\partial X_2} + \psi_1 + \frac{\partial}{\partial X_2}[N(X)]^T \psi_2 \end{bmatrix} \tag{19}$$

$$0 = \frac{\partial L^T}{\partial U} + Z^T(X_1)\psi_2 \tag{20}$$

$$\delta x_0 = \delta x_f = \delta t_f = 0 \tag{21}$$

Eq. (18) and Eq. (19) express the required optimality conditions. The achieved solution is a candidate optimal solution. Since the upper and lower torque limits have been defined by Eq. (20), the torque value of each motor can be obtained from Eq. (22).

$$U = \begin{cases} U^+ & -R^{-1}Z^T\psi_2 > U^+ \\ -R^{-1}Z^T\psi_2 & U^- < -R^{-1}Z^T\psi_2 < U^+ \\ U^- & -R^{-1}Z^T\psi_2 < U^- \end{cases} \tag{22}$$

Which in this relation, high and low limits of torques' value is determined as follows.

$$U^+ = K_1 - K_2 X_2$$
$$U^- = -K_1 - K_2 X_2 \tag{23}$$

Which in Eq. (23) the parameter of $K_1 = \begin{bmatrix} \tau_{s1} & \tau_{s2} & \ldots & \tau_{sn} \end{bmatrix}$ and $K_2 = diag\left[\tau_{s1}/\omega_{m1} & \ldots & \tau_{sn}/\omega_{mn} \right]$ are defined. Regarding that state vectors are fixed at initial and final periods, thus the Eq. (15) takes the form of Eq. (21) and boundary conditions are defined as follows.

$$X_1(0) = X_{10}, \qquad X_2(0) = X_{20}$$
$$X_1(t_f) = X_{1f}, \qquad X_2(t_f) = X_{2f} \tag{24}$$

Here, the Eq. (18) to (24) express three categories of relations.
So the Eq. (18-19) define system's dynamic model. Optimum conditions are obtained by Eq. (22) and boundary conditions by Eq.s (21 and 24).

In order for solving the two-point boundary value problem, iterative algorithm is used. By inserting Eq. (22, 23) in Eq. (18, 19), 4n of differential equation is obtained. 4n of boundary condition is obtained from Eq. (24). So, a two-point boundary value problem is constructed. In this algorithm, the obtained error value from Eq. (7) should be lower than favorite value of ε. Therefore:

$$\frac{1}{2}\left\| X_1(t_f) - X_{1f} \right\|^2 + \frac{1}{2}\left\| X_2(t_f) - X_{2f} \right\|^2 \leq \varepsilon \tag{25}$$

Where in this relation X_f is the favorite value in the final time and X_{t_f} is the calculated state vector value at the final point. The relative significance of position and velocity error value for each of the joints is determined using W_v and W_p matrices. The extreme value of motors capacity (U^- and U^+) is used for determining portable maximum load. So that if the load value exceeds the maximum portable load by the robot, the motor of each joint requires applying a torque greater than the permitted limit which causes the joints' torque to exceed their limits.

Simulation
In this part, we deal with the simulation of a planar two-link dynamic arm with the specifications provided in table (1).

Table 1. simulation parameters (16)

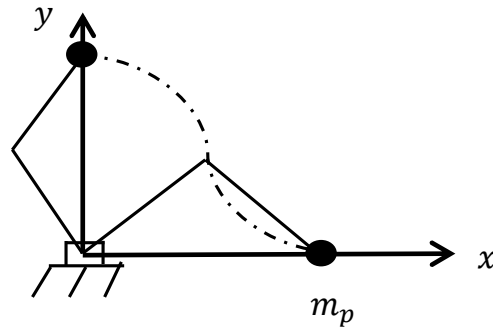| parameter	value
Length of links	$L_1 = L_2 = 1 \quad (M)$
Mass	$m_1 = m_2 = 2, \quad (Kg)$
Moment of inertia	$I_1 = I_2 = 0.166 \quad (Kg.m^2)$
Max. no load speed	$\omega_{s1} = \omega_{s2} = 5.6 \quad (Rad/s)$
Actuator stall torque	$\tau_{s1} = \tau_{s2} = 104 \quad (N.m)$

Fig. (1) shows this robot in the horizontal plane.

Figure 1. Schematic of robot and optimal path (16)

Regarding the reference of (16), the initial position of the end-effector in the XZ plan at $t = 0s$ is $P_0 = (1,0)$ and the final position at $t = 1s$ is $P_f = (0,1.73)$. Moreover, the velocity of final end effector in the beginning and end of the trajectory is zero. Joints' position and velocity values are obtained from inverse kinematic solution as follows.

$$q_{10} = 60°, \; q_{20} = -120°, \; q_{1f} = 120°$$
$$q_{2f} = -60°, \; \dot{q}_{10} = \dot{q}_{20} = \dot{q}_{1f} = \dot{q}_{2f} = 0 \tag{26}$$

State variables of X_1, X_2, and U from Eq. (2) are defined as follows.

$$X_1 = \begin{bmatrix} q_1(t) \\ q_2(t) \end{bmatrix} = \begin{bmatrix} x_1(t) \\ x_3(t) \end{bmatrix} \quad X_2 = \begin{bmatrix} \dot{q}_1(t) \\ \dot{q}_2(t) \end{bmatrix} = \begin{bmatrix} x_2(t) \\ x_4(t) \end{bmatrix}$$
$$U = \begin{bmatrix} u_1(t) \\ u_2(t) \end{bmatrix} \tag{27}$$

Where q_1 and q_2 are the first and second link angles and $\dot{q}_1$, $\dot{q}_2$ show the links angle velocity. u_1 and u_2 show the torque of the first and second link motors. Using Eq. (18), four equations related to dynamic equations state space form is extracted as follows.

$$\dot{x}_1 = x_2, \; \dot{x}_3 = x_4$$
$$\dot{x}_2 = \frac{d_{22}(U_1 - C_1 - G_1)}{d_{11}d_{22} - d_{12}^2} - \frac{d_{12}(U_2 - C_2 - G_2)}{d_{11}d_{22} - d_{12}^2} \tag{28}$$
$$\dot{x}_4 = \frac{-d_{12}(U_1 - C_1 - G_1)}{d_{11}d_{22} - d_{12}^2} + \frac{d_{11}(U_2 - C_2 - G_2)}{d_{11}d_{22} - d_{12}^2}$$

Where d_{ij}, C_i, G_i,: $I, j = 1,2$ is related to two-link robot which is provided in the appendix section. Now, by defining penalty matrices as

$$W_1 = \begin{bmatrix} w_1 & 0 \\ 0 & w_3 \end{bmatrix}; \; W_2 = \begin{bmatrix} w_2 & 0 \\ 0 & w_4 \end{bmatrix}; \; R = \begin{bmatrix} r_1 & 0 \\ 0 & r_2 \end{bmatrix} \tag{29}$$

And by inserting Eq. (28) in Eq. (8), target function:
$$L = 0.5 \times (r_1 u_1^2 + r_2 u_2^2 + w_1 x_1^2 + w_3 x_3^2 + w_2 x_2^2 + w_4 x_4^2) \tag{30}$$

From Eq. (11), Hamiltonian function is obtained as follows.

$$H = L + \psi_1 \dot{x}_1 + \psi_2 \dot{x}_2 + \psi_3 \dot{x}_3 + \psi_4 \dot{x}_4 \qquad (31)$$

Where L and $\dot{x}_i, i = 1,2,3,4$ from Eq. (28) and (30) are inserted. Using Eq. (13) deriving from Hamiltonin function, the equations related to quasi-states are obtained as follows.

$$\dot{\psi}_1 = \frac{-\partial H}{\partial x_1} \;\; ; \;\; \dot{\psi}_2 = \frac{-\partial H}{\partial x_2} \;\; ; \;\; \dot{\psi}_3 = \frac{-\partial H}{\partial x_3} \;\; ; \;\; \dot{\psi}_4 = \frac{-\partial H}{\partial x_4} \qquad (32)$$

Now, using Eq. (14) and deriving form Hamiltonian function in proportion to control values, the following two relations result.

$$\frac{\partial H}{\partial u_1} = r_1 u_1 + \frac{\psi_2 d_{22} - \psi_4 d_{12}}{r_1 (d_{11} d_{22} - d_{12}^2)} = 0,$$

$$\frac{\partial H}{\partial u_2} = r_2 u_2 - \frac{\psi_2 d_{12} - \psi_4 d_{11}}{r_2 (d_{11} d_{22} - d_{12}^2)} = 0 \qquad (33)$$

By solving these equations, the control values are obtained in the acceptable range.

$$u_1 = \frac{-(\psi_2 d_{22} - \psi_4 d_{12})}{r_1 (d_{11} d_{22} - d_{12}^2)} \;\; ; \;\; u_2 = \frac{\psi_2 d_{12} - \psi_4 d_{11}}{r_2 (d_{11} d_{22} - d_{12}^2)} \qquad (34)$$

Therefore, optimum control rule for Eq. (22) is written as follows.

$$U_i = \begin{cases} U_i^+ & u_i > U_i^+ \\ u_i & U_i^- < u_i < U_i^+ \;, i = 1, 2 \\ U_i^- & u_i < U_i^- \end{cases} \qquad (35)$$

Which the limitations of control values of each motor is calculated as follows.

$$U_1^+ = k_{11} - k_{12} x_2 \;\; ; \;\; U_1^- = -k_{11} - k_{12} x_2$$

$$U_2^+ = k_{21} - k_{22} x_4 \;\; ; \;\; U_2^- = -k_{21} - k_{22} x_4 \qquad (36)$$

Where the k_{ij}, i, j = 1, 2 values is calculated from motor specifications provided in table (1).

Determining optimum trajectory of maximum load for two-link manipulator using hypothesis of the article (16)

In this part, for the given two-link manipulator and boundary conditions in reference (16), maximum of load carrying capacity and corresponding optimum trajectory are calculated. Values of W_1 , W_2 , and R are selected in this way. So that $W_1 = W_2 = (0)$ and R= diag (10^{-5} , 10^{-5}). For this manipulator, the given boundary conditions, and intended target function, the obtained maximum load is 5/53 *kg*. In order to show the algorithm performance for calculating maximum load, the results of simulation for five different load values have been presented in diagrams.

In Fig. (2), the position of the end effector in XZ plane for different load values is shown. Figs. (3a) and (3b) show the joints' position with respect to time. Also Figs. (4a) and (4b) variations of angular velocity with respect to time with load carrying variations are shown.
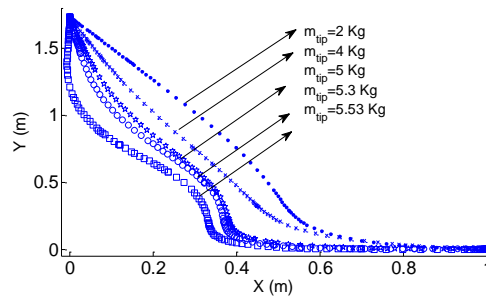
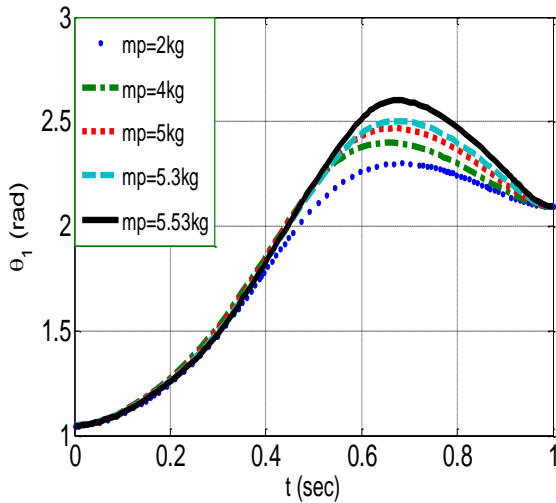Figure 2. End effector trajectory in XY plan

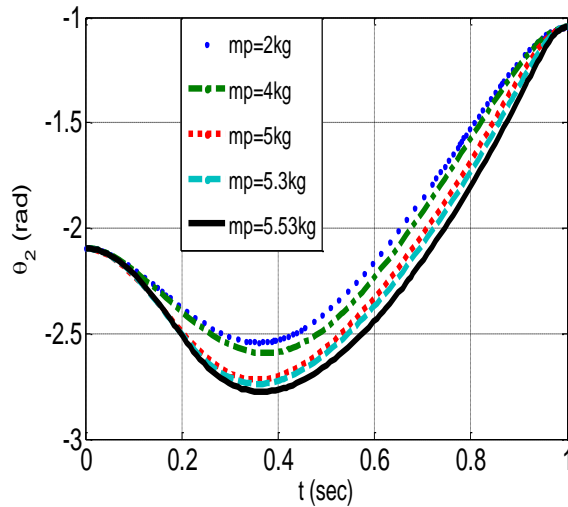Figure 3a. angular position of joint 1

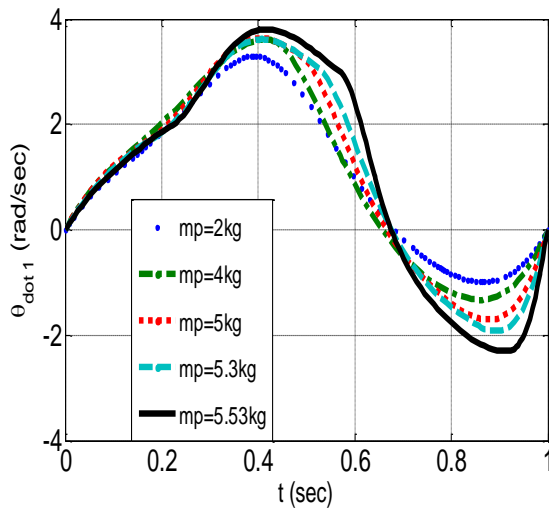Figure 3b. angular position of joint 2
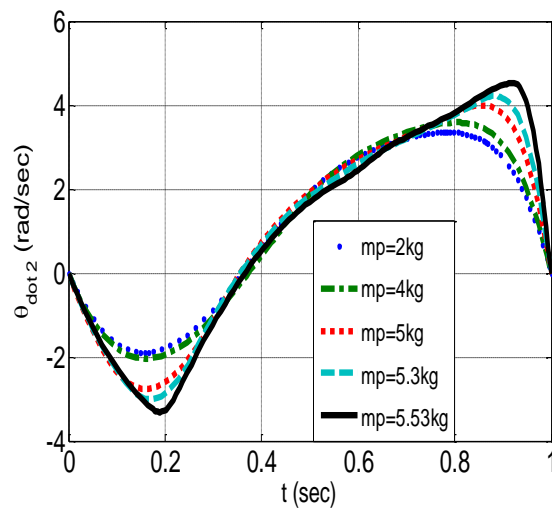

Figure 4a. Angular velocities of joints 1

Figure 4b. Angular velocities of joints 2

In Figs. (5a) and (5b), the diagram of the first and second joint torques in proportion to time for different load values has been shown. As you can see, with the increase of the load, torque values increase too and progress toward torque limits until they reach to their values. As can be seen, the torques have reached saturation for $5/53 \; kg$ load and always are on high and low limits. In this situation, if the load exceeds $5/53 \; kg$, it necessitates the torques to exceed their limits which it is not possible and when the condition (25) is not fulfilled in the problem solution of boundary value, this fact is substantiated. The obtained $m_p = 5.53 \; kg$ is the maximum load carrying capacity for the intended target function. The obtained result is fully consistent with reference (16).
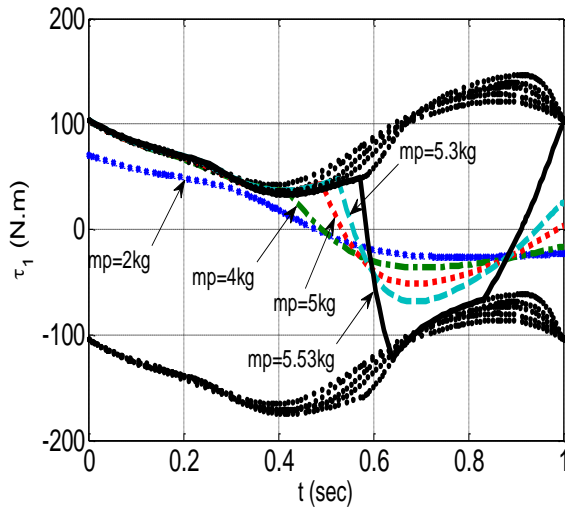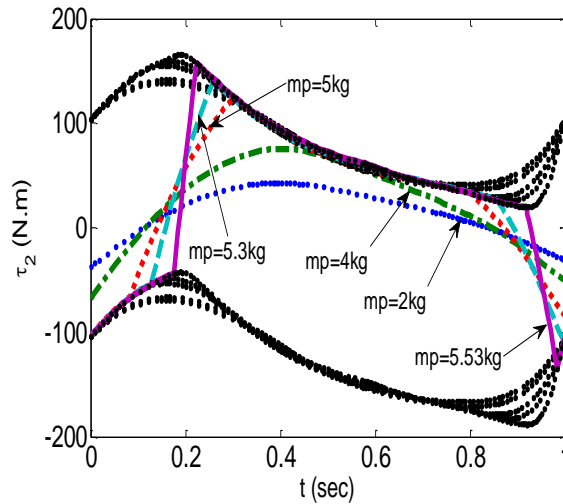
Figure 5a. Torques of joint 1   Figure 5b. Torques of joint 2

Determining the optimum trajectory of two-link manipulator by applying dynamic torque assumption

In Sec. 3 the maximum load and the corresponding optimum trajectory were obtained. In Ref. (16), torque's high and low limits based on a function of robot's joints velocity (Eq. (36)) is considered. Regarding that torque's velocity varies by joints' velocity, in Hamiltonian function it is not derived in proportion to joints' velocity. Here, the aforementioned problem is considered by applying joints' torque limits dynamically. Using Eq. (36), we arrive at the following relation.

$$-k_{11} - k_{12}x_2 \leq U_1 \leq k_{11} - k_{12}x_2 \tag{37}$$

$$-k_{21} - k_{22}x_4 \leq U_2 \leq k_{21} - k_{22}x_4$$

From the above two inequalities, the following four inequalities are obtained.

$$f_{11}(x(t)) = U_1 + k_{11} + k_{12}x_2 \geq 0 \tag{38}$$

$$f_{12}(x(t)) = -U_1 + k_{11} - k_{12}x_2 \geq 0$$
$$f_{21}(x(t)) = U_2 + k_{21} + k_{22}x_4 \geq 0 \tag{39}$$

$$f_{22}(x(t)) = -U_2 + k_{21} - k_{22}x_4 \geq 0$$

Thus, two new state variables are defined as follows (17).

$$\dot{x}_5 = \left(f_{11}(x(t))\right)^2 \text{H}\left(-f_{11}(x(t))\right)$$
$$+ \left(f_{12}(x(t))\right)^2 \text{H}\left(-f_{12}(x(t))\right) \tag{40}$$

$$\dot{x}_6 = \left(f_{21}(x(t))\right)^2 \text{H}\left(-f_{21}(x(t))\right)$$
$$+ \left(f_{22}(x(t))\right)^2 \text{H}\left(-f_{22}(x(t))\right) \tag{41}$$

Where H (x) signifies Heaviside function. So, Hamiltonian function is obtained as follows.

$$H = L + \psi_1 \dot{x}_1 + \psi_2 \dot{x}_2 + \psi_3 \dot{x}_3 + \psi_4 \dot{x}_4 + \psi_5 \dot{x}_5 + \psi_6 \dot{x}_6 \tag{42}$$

Now using derivation from Hamiltonian function in proportion to state and quasi-state variables, two sets of differential equations are obtained as follows (17).

$$\dot{x}_1 = x_2, \; \dot{x}_3 = x_4$$

$$\dot{x}_2 = \frac{d_{22}(U_1 - C_1 - G_1)}{d_{11}d_{22} - d_{12}^2} - \frac{d_{12}(U_2 - C_2 - G_2)}{d_{11}d_{22} - d_{12}^2}$$

$$\dot{x}_4 = \frac{-d_{12}(U_1 - C_1 - G_1)}{d_{11}d_{22} - d_{12}^2} + \frac{d_{11}(U_2 - C_2 - G_2)}{d_{11}d_{22} - d_{12}^2}$$

$$\dot{x}_5 = \left(f_{11}(x(t)) \right)^2 H\left(- f_{11}(x(t)) \right)$$

$$+ \left(f_{12}(x(t)) \right)^2 H\left(- f_{12}(x(t)) \right)$$

$$\dot{x}_6 = \left(f_{21}(x(t)) \right)^2 H\left(- f_{21}(x(t)) \right)$$

$$+ \left(f_{22}(x(t)) \right)^2 H\left(- f_{22}(x(t)) \right)$$

(43)

And quasi-state equations by deriving from Hamiltonian function in proportion to state variables is obtained as follows.

$$\dot{\psi}_1 = \frac{-\partial H}{\partial x_1} \; ; \; \dot{\psi}_2 = \frac{-\partial H}{\partial x_2} \; ; \; \dot{\psi}_3 = \frac{-\partial H}{\partial x_3} \; ; \; \dot{\psi}_4 = \frac{-\partial H}{\partial x_4}$$

$$\dot{\psi}_5 = \frac{-\partial H}{\partial x_5} \; , \; \dot{\psi}_6 = \frac{-\partial H}{\partial x_6}$$

(44)

In Eq. (44), the last two sentences equate zero. Thus, ψ_5 and ψ_6 values will be fixed. By deriving from Hamiltonian function in proportion to control torque of Eq. (34) is obtained as follows.

$$\frac{\partial H}{\partial u_1} = 0 \quad , \quad \frac{\partial H}{\partial u_2} = 0$$

(45)

In order to perform the comparison between the presented method in Ref. (16) and the method offered in this paper, simulation is performed for the two-link robot which a load equal to 2 kg is placed on its end effector. In what follows, the results of simulation are presented in Figs. (6a) to (7b).
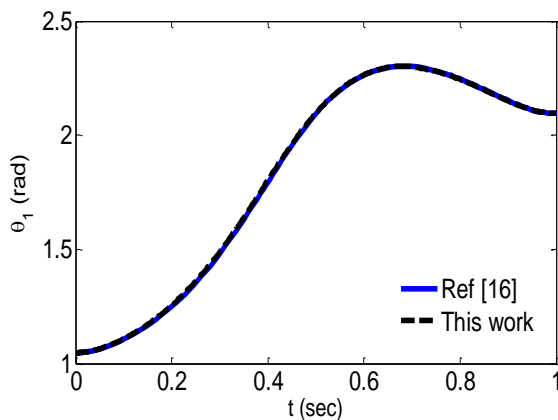

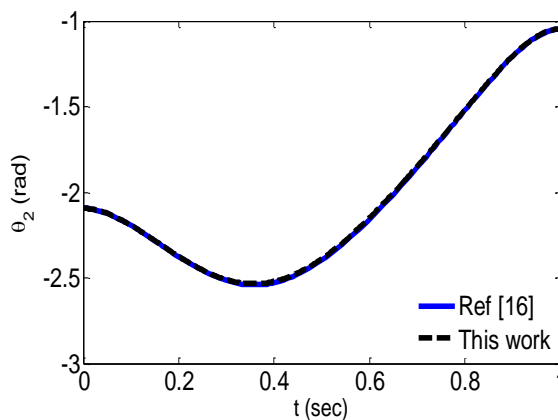Figure 6a. Comparison angular position of joint 1

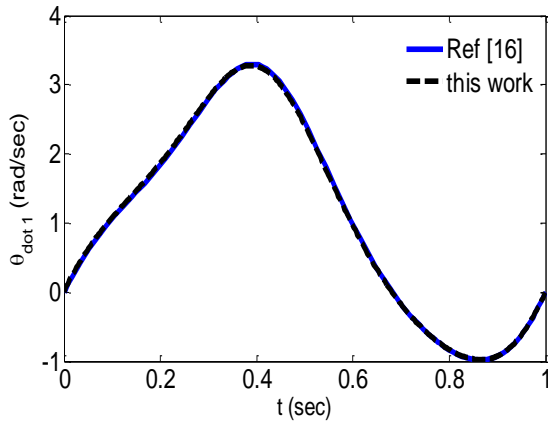Figure 6b. Comparison angular position of joint 2

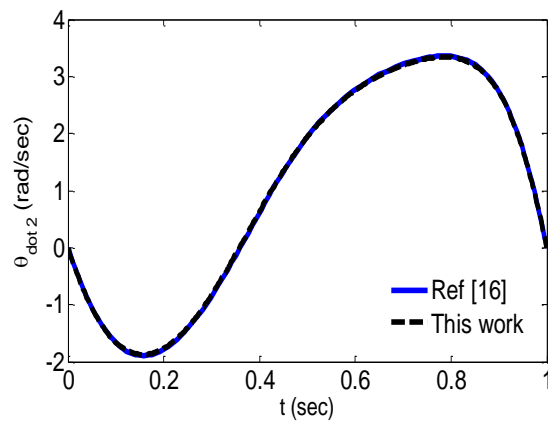Figure 7a. Comparison angular velocity of joint 1

Figure 7b. Comparison angular velocity of joint 2

As is evident from the above diagrams, the position and velocity of both states are similar and diagrams are on each other. Figs. (8a) and (8b) show the torques of first and second joint.
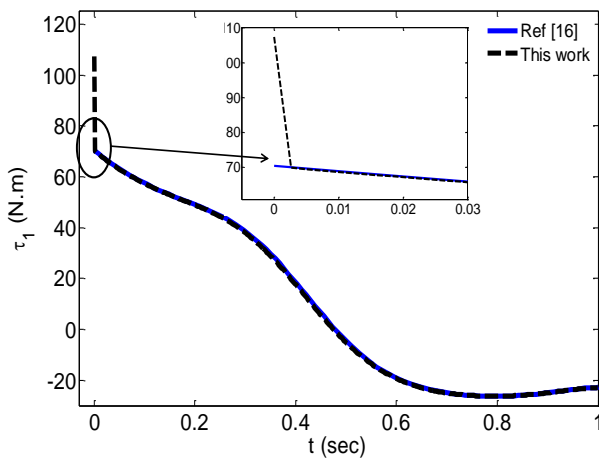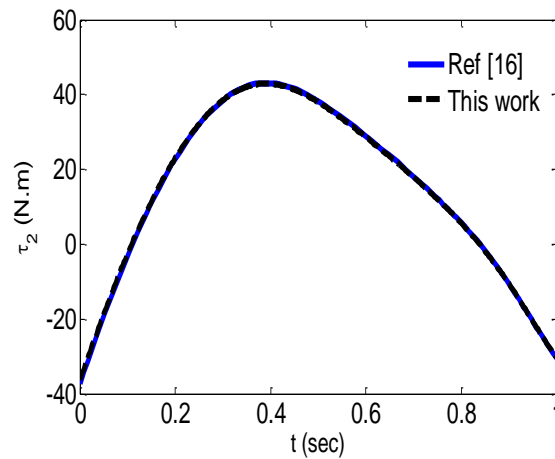

Figure 8a. Comparison torque of joint 1

Figure 8b. Comparison torque of joint 2

First joint torque value (Fig. (8a)) in second method is greater than the first one. This is because in the first method, after the torque value is obtained from Eq. (34), using Eq.s (35-36) the torque value is limited until it reaches saturation, while in the second method high and low limits of joints' torque have been added to Hamiltonian function as unequal constrains. In other words, joints' torques can increase under the influence of angular velocity, while in the method offered in Ref. (16) this was not possible.

CONCLUSIONS

In this article, maximum load carrying capacity of two-link robot has been obtained by open chained optimum control method and employing Ponyeryagen Minimum Principle. Regarding motors' limitations, motors' Torque limitation constrain was applied to the problem. The required conditions of optimality were obtained once by Ref. (16) and another time by dynamic torque assumption. In method Ref. (16), this constrain is not fed into Hamiltonian function, while using a new method which is employed in this article, this constrain has been fed into Hamiltonian function as an inequality and therefore is fed into state and quasi-state equations. The obtained differential equations set along with boundary conditions forms a two-point boundary value equation set which was solved using BVP4C command of MATLAB software. By performing the simulation which was carried out about a planar two-link robot in order to determine maximum load carrying capacity in point- to- point motion, it is shown that joints' position and angular velocity in both states is the same.

Appendix

The motion of manipulator is performed in horizontal plane, therefore, gravity velocity is taken as zero. Inertia matrix of a two- link manipulator is expressed as follows.

$$D = \begin{bmatrix} d_{11} & d_{12} \\ d_{12} & d_{22} \end{bmatrix}$$

$$d_{11} = a_1 + a_2 + 2a_3\cos(q_2) \ , \ d_{12} = a_2 + a_3\cos(q_2)$$

$$d_{22} = a_2$$

In which

$$a_1 = I_1 + m_1 L_{c1}^2 + (m_2 + m_p)L_1^2$$

$$a_2 = I_2 + m_2 L_{c2}^2 + m_p L_2^2$$

$$a_3 = L_1(m_2 L_{c2} + m_p L_2)$$

$$a_4 = m_1 L_{c1} + (m_2 + m_p)L_1$$

$$a_5 = m_2 L_{c2} + m_p L_2$$

Lateral-Coriolis forces of C center and gravity force of G are defined as follows.

$$C = \begin{bmatrix} C_1 \\ C_2 \end{bmatrix} \ ; \ G = \begin{bmatrix} G_1 \\ G_2 \end{bmatrix}$$

In which

$$C = \begin{bmatrix} -a_3\sin(q_2)(2\dot{q}_1\dot{q}_2 + \dot{q}_2^2) \\ a_3\sin(q_2)\dot{q}_1^2 \end{bmatrix}$$

$$G = \begin{bmatrix} g(a_4\cos(q_1) + a_5\cos(q_1 + q_2)) \\ g a_5\cos(q_1 + q_2) \end{bmatrix}$$

Thus, dynamic equations of a two- link robot in the horizon plane are obtained.

REFERENCES

Betts JT. 1998. Survey of numerical methods for trajectory optimization, J. of Guidance Cont. Dyn., Vol. 21, No. 2, p. p. 193–207.

Chettibi T, Lehtihet HE, Haddad M and Hanchi S. 2004. Minimum cost trajectory planning for industrial robots, European J. of Mechanics A/Solids, Vol. 23, p. p. 703–715.

Diehl M, Bock HG, Diedam H and Wieber PB. 2009. Fast Direct Multiple Shooting Algorithms for Optimal Robot Control, Fast motions in Biomechanics and Robotics, Vol. 1, p.p. Jun.

Haddad M, Chettibi T, Hanchi S and Lehtihet HE. 2006. Optimal motion planner of mobile manipulators in generalized point-to-point task, 9th IEEE Int. Workshop on Advanced Motion Control, p. p. 300-306.

Hull DG. 1997. Conversion of optimal control problems into parameter optimization problems, J. of Guidance, Control and Dynamics, Vol. 20, No. 1, p. p. 57-60.

Kirk DE. 1970. Optimal control theory, An Introduction, Prentice-Hall Inc.,

Korayem MH. 2009. Nikoobin, Formulation and Numerical Solution of Robot Manipulators in Point-to-Point Motion with Maximum Load Carrying Capacity, Transaction B: Mechanical Engineering, Sharif University of Technology, Vol. 16. P. p. 101- 109.

Korayem MH and Nikoobin A. 2009. Maximum payload path planning for redundant manipulator using indirect solution of optimal control problem, Int. J. Adv. Manuf. Tech. Vol. 44, p. p. 725-736.

Korayem MH and Ghariblu H. 2004. Maximum allowable load of mobile manipulator for two given end points of end-effector, Int. J. of AMT, Vol. 24, No. 10, p. p. 743 – 751.

Korayem MH and Gariblu H. 2004. Analysis of wheeled mobile flexible manipulator dynamic motions with maximum load carrying capacities, Robotics and Autonomous Systems, Vol. 48, No. 2, p. p. 63-76.

Luus R. 2003. Iterative dynamic programming, Automatica, Vol. 39, No. 7, p. p. 1315-1316.

Miele A. 1975. Recent Advances in Gradient Algorithms for Optimal Control Problems, Journal of Optimization Theory and Applications, Vol. 17, pp. 361–430, Dec.

Pontryagin L, Boltianski V, Gamkrelidze R and Michtchenko E. 1962. Mathematical theory of optimal processes, Inter-science publisher.

Szyszkowski W and Fotouhi R. 2000. Improving time-optimal control maneuvers of two-link robotic manipulators, J. of Guidance, Control and Dynamics, Vol. 23, No. 5, p. p. 888-889.

Wang LT and Ravani B. 1988. Dynamic load carrying capacity of mechanical manipulators-Part 2, J. of Dynamic Sys., Meas. and Control, Vol. 110, p. p. 53-61.

Wang CYE, Timoszyk WK and Bobrow JE. 2001. Payload maximization for open chained manipulator: Finding motions for a Puma 762 robot, IEEE Transactions on Robotics and Automation, Vol. 17, No. 2, p. p. 218-224.

Xin-Sheng GE and Li-Qun CH. 2006. Optimal motion planning for nonholonomic systems using genetic algorithm with wavelet approximation, Applied Mathematics and Computation, Vol. 180, p. p. 76–85.